Available online at www.sciencedirect.com

ScienceDirect

Procedia CIRP 68 (2018) 237 – 241

www.elsevier.com/locate/procedia

19th CIRP Conference on Electro Physical and Chemical Machining, 23-27 April 2018, Bilbao, Spain

Preparation of biomimetic superhydrophobic surface by a facile one-step pulse electrodeposition

Shuzhen Jiang[a,*], Zhongning Guo[a], Glenn Kwabena Gyimah[a], Chuanyun Zhang[a], Guixian Liu[a]

[a]*School of Electromechanical Engineering, Guangdong University of Technology, Guangzhou, 510006, PR China*

* Corresponding author. Tel.: +86-020-39322412; fax: +86-020-39322415. *E-mail address:* piercejiang88@gmail.com

Abstract

Superhydrophobic surfaces in natural world, such as lotus leaves, are commonly attributed to a combination of hierarchical micro/nano structures and low surface energy materials, giving inspiration for the preparation of artificial superhydrophobic surfaces. In this work, with an equivalent electrolytic time of 10 min, superhydrophobic surfaces on copper substrates were prepared by an one-step pulse electrodepositing process with different frequency in an electrolyte containing lanthanum chloride ($LaCl_3$•$6H_2O$), myristic acid ($CH_3(CH_2)_{12}COOH$) and ethanol. Surface morphology, chemical composition and superhydrophobic property were investigated with SEM, EDX, FTIR and contact angle meter. The results show that the as-prepared surfaces have micro/nano dual scale structures mainly consisting of lanthanum myristate ($La[CH_3(CH_2)_{12}COO]_3$). The maximum water contact angle (WCA) is about 160.3°. This method is time-saving and can be easily extended to other conductive materials.

Peer-review under responsibility of the scientific committee of the 19th CIRP Conference on Electro Physical and Chemical Machining

Keywords: Biomimetic; Superhydrophobic; Contact angle; Pulse electrodeposition; Frequency

1. Introduction

Surface wettability is one of the most important properties of solid material. Superhydrophobicity which means that surfaces with a water contact angle (WCA) greater than 150° has attracted considerable attention on fundamental research as well as industrial application due to its unique behavior in the field of self-cleaning, anti-icing, anti-corrosion, water-oil separation[1-4] etc. A rough surface with special micro/nano structures and/or surface chemical composition with low surface free energy are the key factors of superhydrophobicity.

Inspired by some particular plants, such as lotus leaves, rose petals and rice leaves, many processes were developed to fabricate the artificial superhydrophobic surfaces, including, but are not limited to chemical etching, electrochemical etching, solution-immersion, sol-gel processing, femtosecond laser ablation, chemical vapor deposition, electrospinning and hybrid processes[5-11]. However, most of the above mentioned methods involved some disadvantages such as environmentally unfriendly chemical treatments, high vacuum and ultraclean working condition, expensive equipment, or multi-step and time-consuming processing procedures, which limit their practical applications.

Because of its facile, economical and high efficient intrinsic qualities, direct current electrodeposition[12-14] has drawn great interest of researchers in respect of preparation of superhydrophobic surfaces on conductive substrates. Moreover, large-scale fabrication regardless of the geometric shape of the workpieces is a distinct advantage of cathodic deposition in industrial applications. In addition, electrodeposition has an advantage that the surface morphology of the deposition layer can be simply regulated by tuning the electrodeposition parameters such as composition and concentration of the electrolyte, temperature, electrical parameters and processing time.

Compared with the conventional direct current deposition, the pulse electrodeposition has a different forming mechanism and offers a greater control over the structure and properties of electrodeposits by introducing some unique electrical parameters such as frequency and duty ratio. To the best of our knowledge, only a few researches about the fabrication of superhydrophobic surfaces by pulse electrodeposition have

Peer-review under responsibility of the scientific committee of the 19th CIRP Conference on Electro Physical and Chemical Machining
doi:10.1016/j.procir.2017.12.055

been conducted and reported[15]. The relationship between the electrical parameters of pulse current and the morphology of deposition layer, as well as their profound impact on the performance of the wettability need to be revealed systematically.

In this work, a rapid one-step process for fabrication of biomimetic superhydrophobic surface by pulse electrodeposition was presented. The effect of different frequency of pulse current on the surface morphology and wettability was specifically investigated.

2. Experimental

2.1. Materials & sample preparation

Anhydrous ethanol and myristic acid of analytical grade were used as received. Lanthanum chloride ($LaCl_3$•$6H_2O$) was used without further purification. Commercially pure copper sheets with a thickness of 1 mm were used as the substrate material for the deposition of superhydrophobic coatings. Copper plates with a size of 30 mm × 30 mm × 1 mm were abraded with silicon carbide papers (from 800 to 2000 grades), then ultrasonically degreased in anhydrous ethanol for 10 min, followed by ultrasonic cleaning with deionized water for 10 min before being dried under atmospheric condition.

2.2. Pulse electrodeposition

Electrolytic solution was prepared by adding 0.04 M lanthanum chloride and 0.1 M myristic acid into 100 ml ethanol under magnetically stirring at ambient temperature. Two copper plates were taken as the anode and cathode with a distance of 2 cm in an electrolyte cell. Pulse currents of 30 V and 50% duty ratio with different frequency ranging from 50 to 2000 Hz were applied to the two electrodes by using a programmable AC/DC power source (ELGAR SW5250A, USA). The composition of the electrolytic solution and the electrical parameters of the processes are summarized in Table 1, while a schematic diagram of the experimental setup is shown in Fig. 1. In order to avoid contamination and mitigate the effects of the reagent concentration, the electrolyte was replaced by a new solution after fabricating every sample.

After an 10 min equivalent electrolytic time at room temperature under stirring condition (200 rpm) by using a magnetic stirring apparatus, the cathodic electrode was rinsed thoroughly several times with ethanol and distilled water and then was dried in an air condition. Subsequently, a cathodic surface with hierarchical micro/nano structure was obtained.

Table 1. Electrolytic and electrical parameters

Electrolytic Composition	value	Electrical parameters	value
$LaCl_3 \cdot 6H_2O$(M)	0.04	Voltage(V)	30
$CH_3(CH2)_{12}COOH$(M)	0.1	Frequency(Hz)	50, 500, 1k, 2k
$C2H_5OH$(ml)	150	Duty ratio	50%

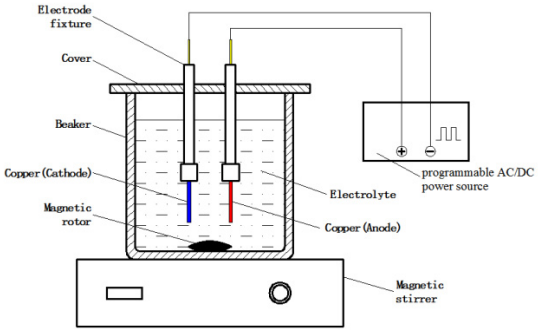

Fig. 1. Schematic diagram of a pulse electrodeposition setup

2.3. Sample characterization

The surface morphology of the as-deposited surfaces was characterized by scanning electron microscopy (SEM, JEOL JSM 6060LV, Japan) at 10 kV. The corresponding chemical composition was examined by Fourier transform infrared spectrophotometer (FTIR, NICOLET 8700, USA) and energy dispersive spectrometer (EDX Genesis 60, USA). Surface wettability was measured by a contact angle measurement instrument (XG-CAMB1, China) at ambient temperature for each surface. Water droplets with about 4 μl were dropped on the deposited layers from a distance of 0.2 cm by vibrating the burette. The reported data were obtained as the average of five measurements at different locations on the sample.

3. Results and discussion

3.1. Surface morphology

Surface morphology plays an important role on the wetting properties of a surface. Fig. 2 shows the SEM images of the as-prepared deposition layers at 30V and 50% duty ratio for various frequency after 10 min equivalent electrolytic time. Fig.2(a) shows the morphology of the cathodic surface obtained under 50 Hz condition. It is clear that flower-like clusters with a diameter around 30-60 μm were formed. These clusters have countless overlapping petals, which makes it similar to the peony flowers. Beneath the flower-like clusters, micro particles with a diameter about 5-15 μm were deposited and distributed relatively uniform. When the frequency is extended to 500 Hz, the SEM images of the surface morphology are shown in Fig.2(b). The flower-like clusters could also be found on the deposited surface. However, the petals of the flower-like structure are looser than the ones shown on Fig.2(a). Around and under the flower-like clusters, particles with a diameter about 5-15 μm were deposited which lead to heterogeneous surface structures.

When the frequency is prolonged to 1000 Hz, the SEM images of the surface morphology are shown in Fig.2(c). The flower-like structure disappeared and only the relatively uniform mastoids with a diameter of around 10 μm were formed. Furthermore, interconnected hair-like nano structure with a dimension of about 1 μm long and 50 nm wide could be observed on the micro-scale asperity structures. Image at higher magnification as shown by the inset of Fig.2(c)

demonstrated that the combination of micro-nano dual scale structure which makes it own a similar characteristic with the surface of lotus leaf. Thus, the surface obtained under this condition exhibited a highly textured morphology with hierarchical micro-nano structure. With increasing frequency to 2000 Hz, the SEM images of the surface morphology are shown in Fig.2(d). Almost all of the micro particles have cracks on the surface, which made them similar to the shape of coffee beans.

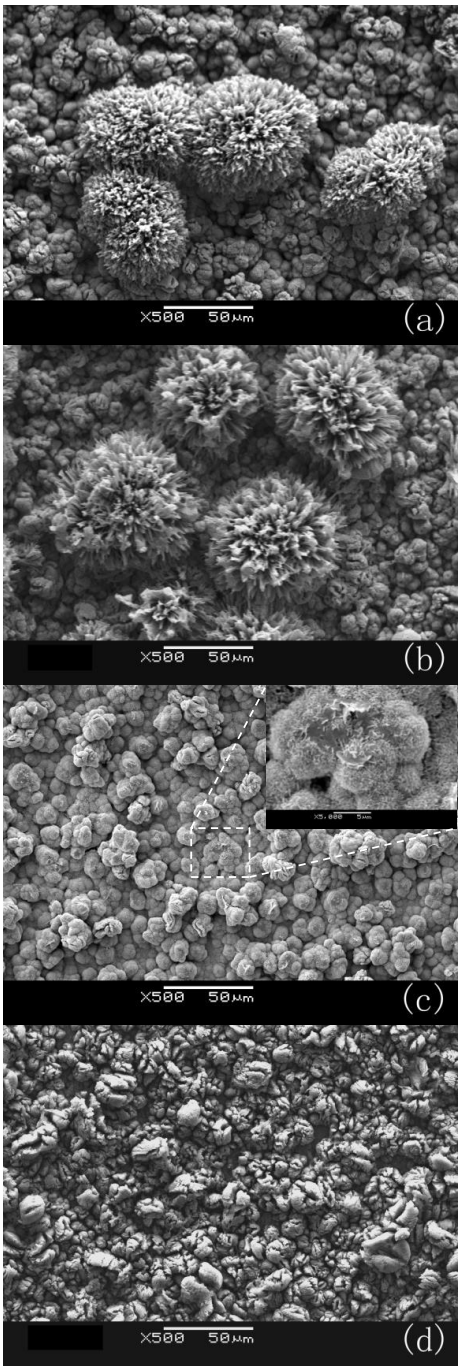

Fig. 2. SEM images of the surfaces deposited at 30V and 50% pulse current for different frequency.(a) 50 Hz; (b) 500 Hz; (c) 1 kHz; (d) 2 kHz.

Electrocrystallization mainly includes three basic steps: generation of seed crystals, formation of crystal nuclei and the growth of crystals. The size of crystalline grains is closely related to the nucleation rate of crystals and growth rate of crystalline grains during the electrocrystallization. When the frequency are 50 Hz and 500 Hz, the cycle of the pulse current are 20 ms and 2 ms and the on-time are 10 ms and 1 ms, respectively. On this occasion, crystal growth plays more important role than the generation of new nucleus, leading to the formation of flower-like structure. When the frequency are 1 kHz and 2 kHz, the cycle of the pulse current are 1 ms and 0.5 ms and the on-time are 0.5 ms and 0.25 ms, respectively. On this occasion, nucleation becomes more pronounced than crystal growth, leading to the disappearance of flower-like structure and only the formation of micro clusters.

3.2. Chemical composition

As shown in Fig. 3, FTIR spectrum was used to get the functional group information of the deposition layer obtained under 1000 Hz. In the low frequency region, the corresponding absorption peak of free carboxyl group (-COO-) from myristic acid appears at 1701 cm^{-1}[16], while the deposition layer exhibits the adsorption peaks at 1526 cm^{-1} and 1440 cm^{-1}. which may stem from asymmetric and symmetric stretches of carboxyl group. In the high frequency region, the absorption peaks at 2849 cm^{-1} and 2915 cm^{-1} are ascribed to methylene groups (-CH_2-)asymmetric and symmetric stretching vibrations while the absorption peaks at 2955 cm^{-1} are attributed to methylene groups (-CH_3) asymmetric stretching vibrations. The surface energy of -CH_3 and the -CH_2- groups are 24 mJ/m^2 and 31 mJ/m^2[17], which indicates that the deposition layers have low free energy.

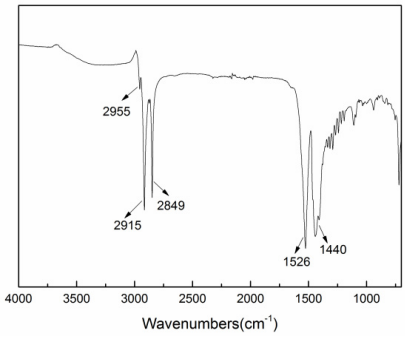

Fig. 3. FTIR spectrum of the superhydrophobic surface obtained by pulse electrodeposition

Table 2. Composition of the as-prepared superhydrophobic surface obtained by EDX.

Element	Wt %	At %
C-K	64.63	84.52
O-K	12.73	12.49
Cl-K	1.31	0.58
La-L	21.33	2.41
Total	100	100

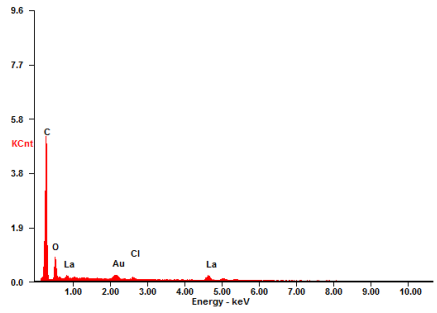

Fig. 4. EDX spectrum of the superhydrophobic surface obtained by pulse electrodeposition

Fig. 4. depicts EDX spectrum and shows that the elements La, C, O and Cl can be observed on the as-prepared surfaces. As shown in table 2, the atom percentage of La/C/O is about 1:35.07:5.18. Hence, it can be inferred that a low surface free energy material named lanthanum myristate ($La[CH_3(CH_2)_{12}COO]_3$) is deposited on the copper substrates.

3.3. Surface wettability

In order to reveal the relationship between the frequency of pulse current and the surface wettability, the contact angles of the as-prepared surfaces were measured and shown in Fig. 5. The contact angle reached 155.5° when employed 50 Hz and the corresponding surface morphology is the one with tight flower-like petals. When the frequency prolonged to 500 Hz, the contact angle decreased slightly to 153.6° and the corresponding surface morphology is the one with loose flower-like petals. As the frequency extended to 1000 Hz, the contact angle increased to 160.3°, reaching the maximum level. It should be noticed that the corresponding surface morphology shown in Fig. 2.(c) demonstrate a highly-textured surface with hierarchical micro-nano dual scale structure which has a similar characteristics with lotus leaf. With increasing frequency to 2000 Hz, the contact angle decrease slightly to 157.1°. The surface obtained under this condition has similar clusters compared with the one obtained under 1000 Hz, but with bigger size and without hair-like structure on the clusters surface. Combined with Fig. 2 and Fig. 5, it can be deduced that the variation of surface morphologies have profound effects on surface wettability.

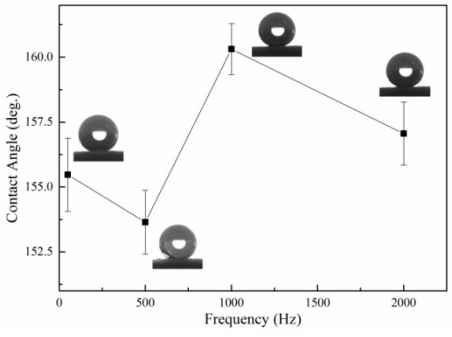

Fig. 5. Relation of water contact angle and pulse current frequency.

4. Conclusion

In conclusion, the fabrication of superhydrophobic surfaces were successfully processed by a rapid one-step pulse electrodeposition with an electrolyte solution containing lanthanum chloride, myristic acid and ethanol. The experimental results show that the frequency of the pulse current plays an important role in determining the surface morphology. It is the combination of a dual micro-nano surface structure and a surface layer of $La(CH_3(CH_2)_{12}COO)_3$ with low surface energy that has contributed to the superhydrophobicity with a contact angle as high as 160.2°. It is expected that this method could be easily extended to various conductive materials for the fabrication of functional surfaces with superhydrophobic properties.

Acknowledgements

This work was supported by National Natural Science Foundation of China (51575113) and China Postdoctoral Science Foundation(2016M600640).

References

[1] Wang G, Liang W, Wang B, Zhang Y, Li J, Shi L, Guo Z. Conductive and transparent superhydrophobic films on various substrates by in situ deposition. Applied Physics Letters 2013; 102: 203703.
[2] Wang N, Xiong D, Lu Y, Pan S, Wang K, Deng Y, Shi Y. Design and fabrication of the lyophobic slippery surface and its application in anti-icing. The Journal of Physical Chemistry C 2016; 120: 11054-11059.
[3] Liu Y, Li S, Zhang J, Liu J, Han Z, Ren L. Corrosion inhibition of biomimetic super-hydrophobic electrodeposition coatings on copper substrate. Corrosion Science 2015; 94: 190-196.
[4] O'Loughlin TE, Martens S, Ren SR, McKay P, Banerjee S. Orthogonal wettability of hierarchically textured metal meshes as a means of separating water/oil emulsions Advanced Engineering Materials 2017; 19: 1600808.
[5] Yang, J, Zhang, Z, Xu, X, Men, X, Zhu, X, Zhou, X. Superoleophobic textured aluminum surfaces. New Journal of Chemistry 2011; 35: 2422-2426.
[6] La DD, Nguyen TA, Lee S, Kim JW, Kim YS. A stable superhydrophobic and superoleophilic cu mesh based on copper hydroxide nanoneedle arrays. Applied Surface Science 2011; 257: 5705-5710.
[7] Zhao L, Liu Q, Gao R, Wang J, Yang W, Liu L. One-step method for the fabrication of superhydrophobic surface on magnesium alloy and its corrosion protection, antifouling performance. Corrosion Science 2014; 80: 177-183.
[8] Kam, D, Bhattacharya, S, Mazumder, J. Control of the wetting properties of an aisi 316l stainless steel surface by femtosecond laser-induced surface modification. Journal of Micromechanics and Microengineering 2012; 22: 105019.
[9] Ishizaki, T, Hieda, J, Saito, N, Saito, N, Takai, O. Corrosion resistance and chemical stability of super-hydrophobic film deposited on magnesium alloy az31 by microwave plasma-enhanced chemical vapor deposition. Electrochimica Acta 2010; 55: 7094-7101.
[10] Grignard B, Vaillant A, Coninck J, Piens M, Jonas AM, Detrembleur C, Jerome C. Electrospinning of a functional perfluorinated block copolymer as a powerful route for imparting superhydrophobicity and corrosion resistance to aluminum substrates. Langmuir : the ACS journal of surfaces and colloids 2010; 27: 335-342.
[11] Lu, Y, Sathasivam S, Song J, Crick CR, Carmalt, C.J, Parkin, I.P. Robust self-cleaning surfaces that function when exposed to either air or oil. Science 2015; 347: 1132-1135.
[12] Liu Y, Yin X, Zhang J, Yu S, Han Z, Ren L. A electro-deposition process for fabrication of biomimetic super-hydrophobic surface and its

corrosion resistance on magnesium alloy. Electrochimica Acta 2014; 125: 395-403.
[13] Liu Y, Liu J, Li S, Han Z, Yu S, Ren L. Fabrication of biomimetic super-hydrophobic surface on aluminum alloy. Journal of Materials Science 2014; 49: 1624-1629.
[14] Chen Z, Hao L, Chen C. A fast electrodeposition method for fabrication of lanthanum superhydrophobic surface with hierarchical micro-nanostructures. Colloids and Surfaces A: Physicochemical and Engineering Aspects 2012; 401: 1-7.
[15] Sivasakthi P, Bapu GR, Chandrasekaran M, Sreejakumari S. Synthesis of a super-hydrophobic ni–ito nanocomposite with pine-cone and spherical shaped micro-nanoarchitectures by pulse electrodeposition and its electrocatalytic application. RSC Advances 2016; 6: 44766-44773.
[16] Wang Y, Wang W, Zhong L, Wang J, Jiang Q. Super-hydrophobic surface on pure magnesium substrate by wet chemical method. Applied Surface Science 2010; 256: 3837-3840.
[17] Robert, F. Coming to an unsticky end. Nature 1994; 368: 16.